A mononuclear cobalt(III) carboxylate complex with a fully O-based coordination sphere: CoIII-O bond homolysis and controlled radical polymerisation from [Co(acac)2(O2CPh)]

Maxime Michelas, Jean-Claude Daran, Alix Sournia-Saquet, Christophe Fliedel, Rinaldo Poli

A mononuclear cobalt(III) carboxylate complex with a fully O-based coordination sphere: Co^{III}-O bond homolysis and controlled radical polymerisation from $[Co(acac)_2(O_2CPh)]$

Received 00th January 20xx,
Accepted 00th January 20xx

DOI: 10.1039/x0xx00000x

Maxime Michelas,[a] Jean-Claude Daran,[a] Alix Sournia-Saquet,[a] Christophe Fliedel,*[a] Rinaldo Poli,*[a,b]

The addition of benzoyl peroxide to $[Co^{II}(acac)_2]$ in a 1:2 ratio selectively produces $[Co^{III}(acac)_2(O_2CPh)]$, a diamagnetic (NMR) mononuclear Co^{III} complex with an octahedral (X-ray diffraction) coordination geometry. It is the first reported mononuclear Co^{III} derivative with a chelated monocarboxylate ligand and an entirely O-based coordination sphere. The compound degrades in solution quite slowly by homolytic Co^{III}-O_2CPh bond cleavage upon warming above 40°C to produce benzoate radicals and can serve as a unimolecular thermal initiator for the well-controlled radical polymerisation of vinyl acetate. Addition of ligands (L = py, NEt_3) induces benzoate chelate ring opening and formation of both *cis* and *trans* isomers of $[Co^{III}(acac)_2(O_2CPh)(L)]$ for L = py under kinetic control, then converting quantitatively to the *cis* isomer, whereas the reaction is less selective and equilibrated for L = NEt_3. The py addition strengthens the Co^{III}-O_2CPh bond and lowers the initiator efficiency in radical polymerisation, whereas the NEt_3 addition results in benzoate radical quenching by a redox process. In addition to clarifying the mechanism of the radical polymerisation redox initiation by peroxides and rationalizing the quite low efficiency factor for the previously reported $[Co^{II}acac)_2]$/peroxide-initiated organometallic-mediated radical polymerisation (OMRP) of vinyl acetate, this investigation provides relevant information on the Co^{III}-O homolytic bond cleavage process.

Introduction

Cobalt(III) complexes with a fully O-based coordination sphere are stronger oxidants than those supported by N-donor ligands. For instance, the standard reduction potentials (E^0 *vs.* SHE) of $[Co^{III}L_6]^{3+}$ (L = H_2O and NH_3, both S = 0 complexes[1, 2] while their reduced $[Co^{II}L_6]^{2+}$ products are both S = 3/2 complexes) are +1.842 V and near zero, respectively.[3, 4] Consequently, the coordination chemistry of Co^{III} with N-based ligands is very rich, whereas isolated and fully characterized mononuclear Co^{III} complexes with an entirely O-based coordination sphere are much less common. These include the above-mentioned $[Co(H_2O)_6]^{3+}$,[5] $[Co(DMSO)_6]^{3+}$ (DMSO = dimethylsulfoxide),[6] a trioxalate complex, $[Co(C_2O_4)_3]^{3-}$,[7] and a variety of tris(β-diketonates), amongst which the ubiquitous and commercially available tris(acetylacetonate), $[Co(acac)_3]$[8-11] (the literature references are restricted to the structural characterisations by X-ray diffraction). The carbonate complex $[Co(CO_3)_3]^{3-}$ has recently been generated electrochemically.[12, 13] A few fully O-donor-supported oligonuclear systems containing carboxylate ligands have also been described, notably $[Co_3O(O_2CR)_6(H_2O)_3]^+$ (*e.g.* R = Me[14] and *t*Bu[15]) and $[Co_8(O_2CMe)_8(OMe)_{16}]$.[16] The so-called "cobalt(III) acetate", widely used in industry as a homogeneous catalyst for hydrocarbon oxidation, has un unclear structure, probably based on oxo-centred Co_3 clusters.[17] Mononuclear Co^{III} complexes with a fully O-based coordination sphere and at least one monocarboxylate ligand in a chelated coordination mode have not yet been reported to the best of our knowledge. It is also interesting to note that, while complexes with a "$Co^{III}O_6$" coordination sphere are known to undergo outer-sphere electron transfer (OSET) processes, little is known about homolytic Co^{III}-O cleavage to generate O-based radicals. Compounds $[Co^{III}(acac)_3]$[18] and $[Co^{III}(salen)(acac)]$[19] were proposed to serve as radical polymerisation initiators under UV photolytic and thermal conditions, respectively, by the proposed generation of acac$^\bullet$ radicals, while the generation of $acacF_3$ radicals by near-UV light irradiation of $[Co^{III}(acacF_3)_3]$ ($acacF_3$ = 1,1,1-trifluoroacetylacetonate), with generation of $[Co^{II}(acacF_3)_2]$, was demonstrated.[20] $[Co^{III}(tmhd)_3]$ (tmhd = 2,2,2,6,6,6-hexamethylheptane-3,5-dionate) was shown to thermally decompose at T > 165 °C by an unknown mechanism.[21]

An O- *vs*. N-based coordination sphere also strongly affects the cobalt-carbon homolytic bond strength in R-Co^{III}/L complexes, with weaker bonds for complexes with O-donor ligands (*e.g.* β-diketonates) and stronger ones in the presence of N- or mixed (O,N)-donors (*e.g.* porphyrin, Schiff bases). Consequently, in organometallic-mediated radical polymerisation (OMRP, Scheme 1),[22-26] an O-based coordination sphere is more suitable for less activated monomers, which generate more reactive

[a] *CNRS, LCC (Laboratoire de Chimie de Coordination), UPS, INPT, Université de Toulouse, 205 route de Narbonne, F-31077 Toulouse, Cedex 4, France.*
[b] *Institut Universitaire de France, 1, rue Descartes, 75231 Paris (France).*

Electronic Supplementary Information (ESI) available: Experimental procedures, characterization data for compound $[Co(acac)_2(O_2CPh)]$ and its thermal decomposition products, DFT-optimized geometries, polymer characterization data, details of the $[Co(acac)_2(O_2CPh)]$-L and BPO-NEt_3 reactions (xxx pages). See DOI: 10.1039/x0xx00000x

radicals and thus yield stronger bonds in the L/Co^{III}-P_n dormant species.[27] In this respect, [$Co^{II}(acac)_2$] has been particularly successful as a moderating L/Co^{II} species for less activated monomers such as vinyl carboxylates[28-37] or vinylidene dlifluoride.[38, 39] Conversely, complexes with N-based ligands such as porphyrins and Schiff bases inhibit the polymerisation of these monomers, but satisfactorily control the chain growth of more reactive monomers such as (meth)acrylates and styrenics.[27, 40, 41] The polymerisations are typically initiated by either a well-defined organometallic compound with a fragile Co^{III}-R_0 bond (direct initiation)[42] or a conventional radical initiator (I) such as a diazo compound in the presence of the moderating L/Co^{II} complex (reverse initiation).[28]

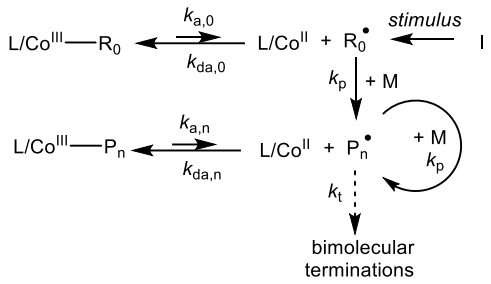

Scheme 1. Initiation and moderating equilibrium of R_n-Co^{III}/Co^{II} in OMRP. L/ = coordination sphere; M = monomer; I = initiator (generating a primary radical $R_0^•$ under any kind of stimulus, *e.g.* thermal, photochemical, redox, mechanical); P_n = polymer chain (= R_0M_n); k_a, k_{da}, k_p, k_t = activation, deactivation, propagation and termination rate constants.

In 2006, Bryaskova *et al.* introduced the combination of benzoyl peroxide (BPO) or lauryl peroxide (LPO) and [$Co^{II}(acac)_2$] as a redox initiating system for the OMRP of vinyl acetate (VAc).[43] The same system was later applied to initiate the controlled polymerisation of acrylic esters,[44] of other vinyl esters[45, 46] and of vinylidene fluoride.[39] This strategy allows avoiding the tedious preparation of the fragile [$(acac)_2Co^{III}$-R_0] complex (R_0 = short PVAc chain)[42] for direct initiation or using the thermally unstable V-70 diazo initiator in combination with [$Co^{II}(acac)_2$] for reverse initiation, but is affected by a quite low initiation efficiency (ca. 10%), which has not been satisfactorily rationalized. The generally accepted radical initiation mechanism[47, 48] for the combination of a peroxide and a reducing metal complex is as illustrated in equations 1-2; Mt = generic metal, L/ = coordination sphere). However, none of the above-mentioned investigations, nor other ones dealing with Co^{II}/peroxide-initiated free radical polymerisations,[49-54] could elucidate the nature of the Co^{III} species produced by reaction 1.

$$ROOR + L/Mt^{n+} \rightarrow RO^- + RO^• + L/Mt^{n+1} \quad (1)$$
$$L/Mt^{n+} + RO^• \rightarrow RO^- + L/Mt^{n+1} \quad (2)$$

In the present contribution, we reveal that the stoichiometric reaction between [$Co(acac)_2$] and BPO (2:1 ratio) provides a simple, efficient and high yielding entry by one-electron oxidative addition into [$Co^{III}(acac)_2(O_2CPh)$], the first mononuclear derivative of Co^{III} with a chelated carboxylate ligand and supported by a fully O-based coordination sphere. We also demonstrate the ability of this bench-stable derivative as a single-component initiator for the OMRP of VAc, describe initial investigations on the addition of ligands (L) to open the carboxylate chelate ring and generate [$Co^{III}(acac)_2(O_2CPh)(L)$], and provide a rationalisation of the reported low efficiency of the [$Co^{II}(acac)_2$]/ROOR initiating system.

Results and Discussion

(a) Synthesis and characterisation of [$Co(acac)_2(O_2Ph)$]

Commercially available and inexpensive [$Co^{II}(acac)_2$] rapidly reacts with BPO in toluene at room temperature in a 2:1 molar ratio to produce [$Co^{III}(acac)(O_2CPh)$] in high yields. Although the compound synthesis requires inert atmosphere conditions, the isolated product is air stable in the solid state, with no sign of alteration over several days as verified by ^{1}H NMR.

In this reaction, the sparingly soluble pink [$Co^{II}(acac)_2$] disappears to produce a deep green solution of the product, the diamagnetism of which is indicated by the sharp ^{1}H and ^{13}C NMR spectra (Figure S1 and Figure S2). The presence of three ^{1}H resonances in a 2:6:6 ratio for the acac H (δ 5.29) and Me (δ 2.04, 1.79) protons indicates asymmetry, consistent with the *cis* arrangement in a C_2-chiral octahedral geometry, as confirmed by a single-crystal X-ray diffraction investigation (Figure 1, Table S1, Table S2). Although of the structure is of relatively poor quality (see Figure S3), it confirms the compound stoichiometry and stereochemistry. Incidentally, this appears to be the first X-ray structure for a heteroleptic Co^{III} mononuclear complex supported by a fully O-based coordination sphere. The mechanism leading to the formation of [$Co^{III}(acac)(O_2CPh)$] is presumably as indicated by equations 1 and 2, but reaction 1 most probably occurs via coordination of one BPO carbonyl function and inner-sphere electron transfer (ISET), rather than by outer-sphere electron transfer (OSET), followed by O-O bond cleavage to directly produce a molecule of product and a benzoate radical. Likewise, the second step (equation 2 for L/Mt^{n+} = [$Co(acac)_2$] and R = Ph) probably involves direct addition of the intermediate $PhCOO^•$ radical to [$Co^{II}(acac)_2$], rather than an OSET. A UV/visible monitoring of the reaction (Figure S4) shows complete conversion in less than 10 h at room temperature.

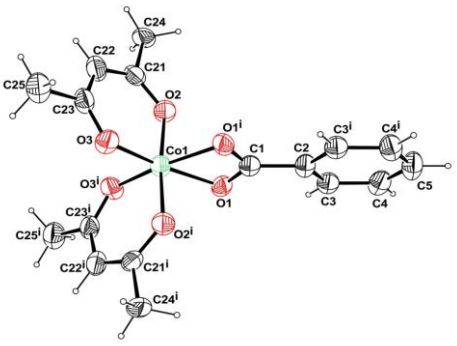

Figure 1. View of the [$Co^{III}(acac)_2(O_2CPh)$] molecule with the atom labelling scheme. Ellipsoids are drawn at the 30% probability level and the H atoms are represented as small circle of arbitrary radii.

Electrochemical measurements (SWV in Figure S5 and CV in Figure S6) show that [$Co^{III}(acac)_2(O_2CPh)$] is much more easily

reduced ($E_{p,c}$ = -0.90 V *vs.* Fc) than [$Co^{III}(acac)_3$] ($E_{p,c}$ = -1.33 V *vs.* Fc). After reduction, a reoxidation wave at much higher potential ($E_{p,a}$ = 0.15 V *vs.* Fc) becomes clearly visible only at high scan rate (Figure S7). The Δ*V* between the two waves is similar to that observed for [$Co^{III}(acac)_3$] and other related Co^{III} tris(β-diketonates),[55] for which this Δ*V* was attributed to a spin state change to 3/2 after reduction.[56]

A variable temperature ^{1}H NMR investigation in C_6D_6 reveals a line broadening phenomenon between 25 and 80 °C, possibly consistent with a dynamic configuration inversion, *e.g.* via a Bailar twist. However, the line broadening is not fully reversible upon cooling, suggesting partial decomposition with generation of a paramagnetic species (Figure 2). This phenomenon suggests reversibility for equation 2 at higher temperatures with generation of PhCOO•.

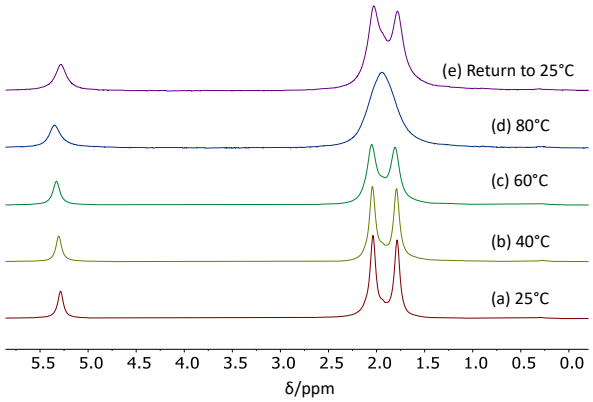

Figure 2. Temperature dependence of the acac ^{1}H NMR resonances for [$Co^{III}(acac)_2(O_2CPh)$] in C_6D_6.

(a) Benzoate radical generation

Additional ^{1}H NMR investigations in C_6D_6 at constant temperature revealed slow decomposition at 60°C, resulting in the deposition of [$Co(acac)_2$] crystals overnight, whereas no decomposition was evident after 16 h at 40 °C or upon standing at room temperature for 3 days in daylight, see Figure S8 and photos in Figure S9. The compound also decomposes in the solid state upon warming above 180°C, hampering the determination of a melting point. A comparative GC-MS investigation of the thermal decomposition products generated from [$Co^{III}(acac)_2$-(O_2CPh)] and BPO in both C_6D_6 (Figure S10) and CH_2Cl_2 (Figure S11) demonstrates the generation of PhCOO• and Ph•, the latter resulting from the decarboxylation of the former,[57-59] through the observed formation of benzoic acid and toluene (see also Scheme S1 and related discussion). The lifetime of the benzoate radical with respect to the decarboxylation to phenyl radical was shown to be in the timescale of microseconds.[60, 61]

The aptitude of [Co^{III}(acac)(O_2CPh)] to liberate PhCOO• was probed by DFT calculations (computational details in the SI). The optimized geometry matches well the observed one (Table S2). The bond cleavage process was investigated in detail for the lighter [Co^{III}(acac)(O_2CMe)] as a model system, to save computational time. In agreement with the NMR evidence, the complex is most stable as a spin singlet with the triplet located 8.2 kcal mol^{-1} higher in Gibbs energy at 25 °C (8.0 kcal mol^{-1} at 60 °C). The triplet complex has an overall *cis*-octahedral geometry, like the singlet. The most interesting difference is a desymmetrisation of the chelating benzoate ligand (Co-O = 1.949, 1.949 Å in the singlet, 1.938, 2.258 Å in the triplet; C-O = 1.270, 1.270 Å in the singlet, 1.246, 1.288 Å in the triplet). The O atom with the shorter Co-O distance has the longer C-O distance, indicating a rearrangement along the path toward monodentate acetate coordination. Other structural differences can be appreciated by comparing the parameters in Table S2.

The liberation of the MeCOO• radical from the model [Co^{III}(acac)(O_2CMe)] complex was computationally probed as a two-step reaction, namely acetate chelate ring opening followed by Co^{III}-O bond homolysis (Figure 3). However, the putative 5-coordinate intermediate could only be optimized in the singlet state, yielding a relatively high-energy square pyramidal geometry with an axial κ^1-OCOMe. Attempted optimisations of a triplet spin isomer with either a square pyramidal or a trigonal bipyramidal geometry converged to the already optimized 6-coordinate chelated structure. This suggests that the homolytic Co-O_2CMe bond cleavage to yield [$Co(acac)_2$] (known to have a quartet spin state, S = 3/2)[62] occurs from the higher-energy triplet in a one-step, spin conserving process (from S = 1 to 3/2-1/2). The overall Gibbs energy cost is 28.3 kcal mol^{-1} under standard conditions (26.6 kcal mol^{-1} at 60 °C), or 20.1 kcal mol^{-1} from the excited state triplet. On the enthalpy scale, the overall cost at 60 °C is 41.5 kcal mol^{-1} (18.6 kcal mol^{-1} from the 6-coordinate triplet intermediate). The overall bond breaking energy was also estimated for the release of the PhCOO• radical from [$Co^{III}(acac)_2(O_2CPh)$], yielding very similar numbers (Δ*G* = 28.8 and 27.1 kcal mol^{-1} at 25 and 60 °C; Δ*H* = 42.3 and 42.2 kcal mol^{-1} at the same two temperatures). These numbers are consistent with the relatively good thermal stability of the compound, but not inconsistent with a significant rate of radical production.[63, 64] For comparison, homolytic bond cleavage was experimentally observed and kinetically investigated for R-Cr^{III}_{aq} complexes ($\Delta H_a^{\ddagger}$ up to 40 kcal mol^{-1})[65-68] and for [R_F-$Mn^{I}(CO)_5$] complexes with R_F = fluorinated alkyl ligands ($\Delta H_a^{\ddagger}$ up to 53.8 kcal mol^{-1} for R_F = CF_3).[69]

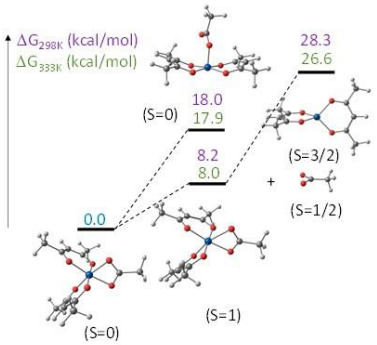

Figure 3. Gibbs energy diagram of the [$(acac)_2Co^{III}$-O_2CMe] bond cleavage.

(b) Initiation of vinyl acetate radical polymerisation

The generation of PhCOO• radicals from [Co^{III}(acac)(O_2CPh)] was also experimentally proven by the successful thermal initiation of a bulk VAc polymerisation, at a temperature as low as 30 °C, with [Co^{III}(acac)(O_2CPh)] as unimolecular initiator. Addition of TEMPO after 24 h quenched the polymerisation (Figure S13a),

demonstrating its radical character. Higher-quality polymers were obtained when 25% of the moderating [$Co^{II}(acac)_2$] complexes was added to the initial mixture. The polymerisation is faster at higher temperatures, the molar mass increases linearly with conversion and the dispersity is relatively low (see Table 1 and Figure S13), as typically observed in OMRP when using [$Co^{II}(acac)_2$] as moderator.[28-38] An ESI-MS analysis of the isolated polymer, Figure S14 shows six major populations of chains, the formation of which is interpreted as shown in Scheme 2 (see the Supporting Information for additional discussion). This type of analysis was not presented in the previously reported VAc polymerisation with [$Co^{II}(acac)_2$]/BPO redox initiation, which is expected to yield the same moderating species. A comparison of experimental and simulated isotopic envelopes for each family of chains is available in Figure S15. This indicates the presence of both PhCOO- and Ph- groups at the α chain end, confirming the formation of free PhCOO$^\bullet$ in a first step, followed by its partial decarboxylation, rather than a concerted Co^{III}-O and C-C bond cleavage. In other words, the aptitude of the benzoate radical to decarboxylate cannot be the driving force for the [$Co^{III}(acac)(O_2CPh)$] decomposition. The initiator efficiency is quite low, but becomes greater at higher temperatures and with increasing conversions, see Table 1.

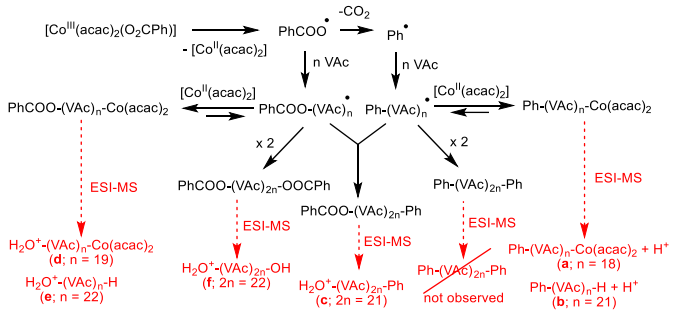

Scheme 2. Initiation mechanism of the VAc polymerisation, and relationship with the chains observed by ESI-MS.

Table 1. Results of the VAc polymerisation initiated by [$Co^{III}(acac)_2(O_2CPh)$].[a]

T/°C	t/h	VAc conv. /%	M_n/g mol^{-1}	f [c]	$Đ$ [d]	k_{obs}/s^{-1} [b]
30	23.2	13.4	20200	0.091	1.13	$4.33\cdot10^{-6}$
	38	28.0	34900	0.098	1.13	
	62	53.0	54100	0.113	1.25	
40	7	14.8	21000	0.095	1.12	$2.41\cdot10^{-5}$
	8	20.4	25100	0.103	1.13	
	15.5	60.4	53800	0.129	1.23	
50	2	13.17	12500	0.141	1.14	$7.19\cdot10^{-5}$
	3.5	47.6	37800	0.147	1.15	
60	0.4	70.1	39400	0.203	1.44	$3.36\cdot10^{-4}$
60 [e]	5	85.9	63700	0.151	2.02	$1.09\cdot10^{-4}$

[a] Conditions: bulk, [VAc]/[Co^{III}]/[Co^{II}] = 126/1/0.25. [b] Determined from the slope of the first-order monomer decay plot (after the initial induction time, *e.g.* see Figure S13). [c] Ratio between the observed and theoretical polymer molar masses. [d] $Đ = M_w/M_n$. [e] In the presence of 30 equiv of pyridine.

The very different stability observed for the title compound in the absence (stable at 40°C) and presence of monomer (initiation at 30°C) can be easily rationalized by the PhCOO$^\bullet$ radical need to diffuse away from the {[$Co^{II}(acac)_2$],PhCOO$^\bullet$} caged pair (k_{diff}, Scheme 3) in order to terminate bimolecularly, whereas it can immediately add to the monomer present at the solvent cage walls under the bulk polymerisation conditions. The resulting VAc-based radical is then trapped, within the solvent cage, by [$Co^{II}(acac)_2$] to establish the OMRP equilibrium for controlled chain growth. The DFT calculations indicate that the [$Co^{III}(acac)_2$(PVAc)] dormant chains are more readily reactivated ($\Delta G_{333.15}$ = 3.9 and 7.2 kcal mol^{-1} for the carbonyl chelate ring opening and Co^{III}-C homolytic bond cleavage, respectively, for a total of 11.1 kcal mol^{-1}). Thus, the PVAc radical chains are generated slowly, then propagate faster, rationalizing quite well the observed low initiation efficiency and its increase with conversion and with temperature.

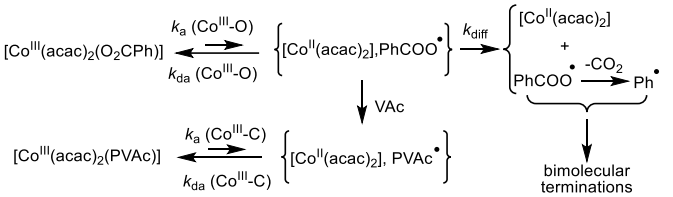

Scheme 3. Mechanism of [$Co^{III}(acac)_2(O_2C$+Ph)] decomposition and VAc polymerisation initiation.

The previously reported polymerisations with redox initiations by [$Co^{II}(acac)_2$]/(BPO or LPO)[43] can now be explained as follows. The first step (equation 1) generates one molecule of [$Co^{III}(acac)_2(O_2CPh)$] and one PhCOO$^\bullet$ radical. The latter can then encounter either a monomer molecule to start a chain propagation, which is then moderated by the OMRP equilibrium, or a second [$Co^{II}(acac)_2$] molecule to yield a second [$Co^{III}(acac)_2(O_2CPh)$] molecule (equation 2). The generated [$Co^{III}(acac)_2(O_2CPh)$] can further be reactivated, but only very slowly as demonstrated in the present contribution. Thus, the efficiency factor in the [$Co^{II}(acac)_2$]/peroxide-initiated polymerisation is generally a little higher (*e.g.* $0.15 \le f \le 0.25$ for [$Co^{II}(acac)_2$]/lauryl peroxide)[43] than in the [$Co^{III}(acac)_2(O_2CPh)$]-initiated polymerisation.

(c) Benzoate chelate opening with donors

Previous work on the OMRP of VAc, with support of DFT calculations, has shown that the addition of neutral ligands (L, notably pyridine and NEt_3)[29, 70] accelerates the polymerisation because the moderating Co^{II} species is stabilized by ligand addition to form a bis-adduct, [$Co^{II}(acac)_2L_2$], to a greater extent than the dormant species, which can only form a monoadduct [$Co^{III}(acac)_2(L)$(PVAc)]. Thus, it was of interest to probe the effect of ligands on the initiating ability of complex [$Co^{III}(acac)_2(O_2CPh)$] in terms of chelate ring opening and homolytic Co^{III}-O_2CPh bond cleavage.

As shown by a ^{1}H NMR investigation, addition of 1 equivalent of pyridine to [$Co^{III}(acac)_2(O_2CPh)$] resulted in an incomplete consumption of the starting compound and in the formation of both *cis* and *trans* [$Co^{III}(acac)_2(O_2Ph)(py)$], see Figure 4 and Figure S16, but further treatment with an excess (3 equivalents) and a longer reaction time resulted in the complete disappearance of [$Co^{III}(acac)_2(O_2CPh)$] and in the full and clean conversion of the *trans* ligand adduct into the *cis* one. The two isomers could be clearly distinguished on the basis of the

number of acac ligand resonances, which are related to the symmetry (one CH and one Me resonance for the C_{2v} *trans* isomer; two CH and four Me resonances for the C_1 *cis* isomer). Closer inspection of the aromatic region of the ^{1}H NMR spectrum (Figure S16b) also revealed broad resonances for the excess free pyridine, suggesting rapid exchange between the free and coordinated ligand, though the independent observation of relatively sharp resonances for all coordinated pyridine protons shows that the system is in the slow-exchange, decoalesced region at room temperature. The ^{13}C NMR analysis of the final product (Figure S17) confirmed the selective production of *cis*-[Co^{III}(acac)$_2$(O$_2$CPh)(py)].

The corresponding interaction with NEt$_3$, on the other hand, left the majority of the starting [Co^{III}(acac)$_2$(O$_2$CPh)] complex unreacted, even after 3 days in the presence of with 3 equiv of the ligand, indicating reduced stability for the NEt$_3$ adduct with a monodentate benzoate. Furthermore, the reaction was not as selective as that with pyridine: the formation of several products, the structure of which remains unclear, was revealed by the complexity of the ^{1}H NMR spectrum in the acac CH and Me regions (Figure S18).

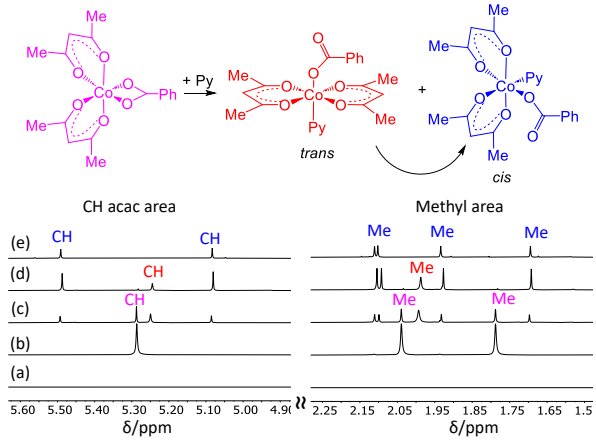

Figure 4. ^{1}H NMR (400 MHz) investigation of the interaction between [Co^{III}(acac)$_2$(O$_2$CPh)] and pyridine. Solvent = C_6D_6. (a) Pyridine. (b) [Co^{III}(acac)$_2$(O$_2$CPh)]. (c) As (b), immediately after addition of pyridine (1 equiv). (d) As (c), immediately after addition of 2 more equiv of pyridine. (e) As (d), after 3 days at room temperature. For the full spectra, see Figure S16.

Additional DFT calculations (Figure 5) gave results in agreement with the above observations. Once again, a model acetate ligand was used for these calculations, whereas the ligands were not simplified. The chelate opening is exoergic for both ligands and pyridine leads to greater stabilisation. Furthermore, the *cis* product is in both cases more stable than its *trans* isomer, by 2.0 and 0.8 kcal mol^{-1} for L = py and NEt$_3$, respectively.

Homolytic cleavage of the Co^{III}-O$_2$CMe bond in *cis*-[Co^{III}(acac)$_2$(O$_2$CMe)(L)] leads to a 5-coordinate [Co^{II}(acac)$_2$(L)] complex in a high spin state (S = 3/2). For both L derivatives, the geometry converged to a slightly distorted square pyramid, even though using a trigonal bipyramidal guess geometry, as previously optimized for other similar derivatives (*e.g.* L = H$_2$O, NH$_3$, MeCOOMe, NMe$_3$, MeCN, DMF, DMSO and also pyridine) but with a different functional.[29, 31] The derivative with L = 1-aminopyridine has been structurally characterized and adopts a distorted square pyramidal geometry,[71] as does the isoelectronic complex [Co^{II}(Ph$_2$MeAsO)$_4$(ClO$_4$)]$^+$ClO$_4^-$.[72] The Co^{III}-O$_2$CMe bond dissociation Gibbs energy in *cis*-[Co^{III}(acac)$_2$-(O$_2$CMe)(L)] is greater than that in the ligand-free [Co^{III}(acac)$_2$-(O$_2$CMe)] for L = pyridine, but smaller for L = NEt$_3$ (*cf.* Figure 5 with Figure 3). The increased bond strength for the pyridine adduct results from the greater stabilisation of the Co^{III} complex (by 10.3 kcal mol^{-1} at room T, associated to the chelate opening and replacement of the carbonyl donor by the py ligand) than of the Co^{II} product (by 7.9 kcal mol^{-1} at room T, associated to the addition of one py ligand to [Co^{II}(acac)$_2$]). For L = NEt$_3$, on the other hand, the Co^{III} system is stabilized by only 5.8 kcal mol^{-1} at room T and the Co^{II} product by as much as 11.4 kcal mol^{-1}.

The Co^{II} moderating species is further stabilized by addition of a second L molecule, to yield *trans*-[Co^{II}(acac)$_2$(L)$_2$], also in a high-spin S = 3/2 configuration. This configuration has been experimentally demonstrated by X-ray diffraction, for instance, for L = DMF and DMSO.[30] The L addition to convert [Co^{II}(acac)$_2$-(L)] to *trans*-[Co^{II}(acac)$_2$(L)$_2$] provides an essentially equivalent stabilization to both systems (11.1 and 10.5 kcal mol^{-1} at room T for L = py and NEt$_3$, respectively).

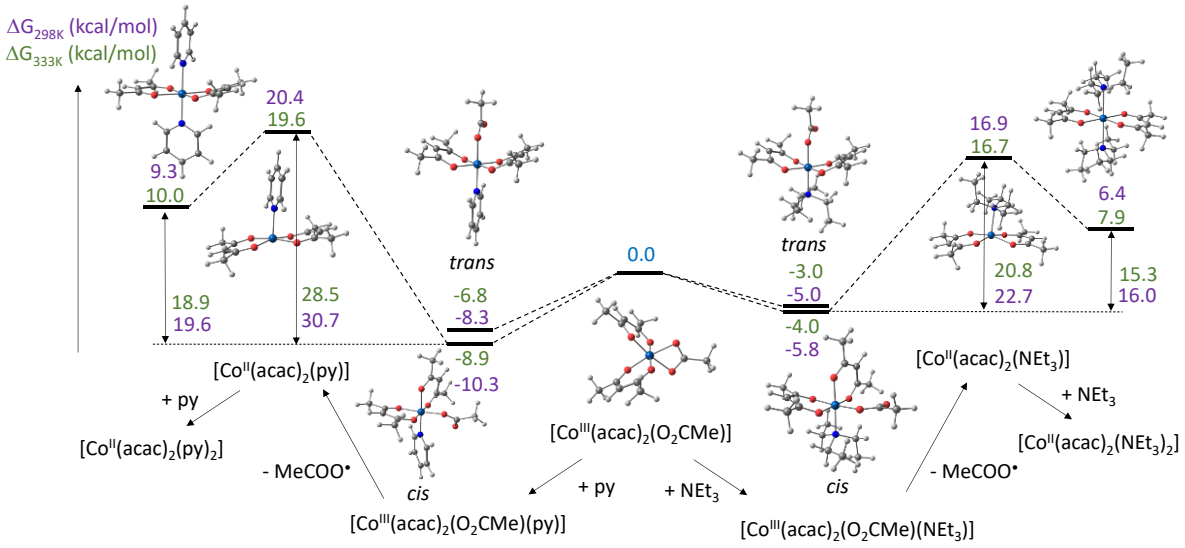

Figure 5. Gibbs energy diagram for the pyridine addition to [$Co^{III}(acac)_2(O_2CMe)$] and for the [$(acac)_2(py)Co^{III}$-O_2CMe] bond cleavage and py addition to [$Co^{II}(acac)_2(py)$].

(d) VAc polymerisation initiated by [$Co^{III}(acac)_2(O_2CPh)$]/L

A repeat of the same experiment in Table 1 at 30°C in the presence of 30 equivalents of pyridine did not produce any polymer over a period of 24 h. A polymer was produced at 60°C, but at a slower rate, with a lower initiation efficiency and with a broader molar mass distribution than the corresponding polymer obtained in the absence of pyridine (see Table 1; polymer GPC in Figure S19), showing that the presence of pyridine slows down the initiation step. This behaviour is consistent with the results of the DFT investigation. As previously demonstrated,[29, 31] the polymerisation is accelerated by ligand coordination because the polymerisation rate is proportional to the rate constant of the radical addition to monomer (a kinetic parameter) and to the equilibrium constant of the [$(acac)_2Co^{III}$-PVAc] activation (a thermodynamic parameter), which is the bond cleavage equilibrium yielding the moderating species [$Co^{II}(acac)_2(py)_2$] and the polymer chain radical. The initiation step, on the other hand, involves the Co^{III}-O_2CPh bond cleavage as the slow (rate-limiting) step, prior to reaching the pyridine-stabilized [$Co^{II}(acac)_2(py)_2$] species. Thus, the initiation is slower in the presence of pyridine (from *cis*-[$Co^{III}(acac)_2(O_2CPh)(py)$] to [$Co^{II}(acac)_2(py)$] plus the benzoate radical) than in its absence, as suggested by the calculated bond dissociation energies for the acetate model (*cf.* Figure 5 with Figure 3).

The VAc polymerisation was also tested with initiation by [$Co(acac)_2(O_2CPh)$] in the presence of NEt_3, because the DFT investigation predicts a faster initiation. However, a repeat of the same experiment in Table 1 at 30°C with the additional presence of 30 equivalents of NEt_3 gave no polymer. The reason of this outcome cannot be the same as in the case of pyridine. Further investigations demonstrated that the reason in this case is the interference of NEt_3 with the initiation step by quenching the benzoate radicals, which are thus unable to add to the VAc monomer and initiate the polymerisation. This is demonstrated by a control experiment, where BPO was exposed to an excess of NEt_3 in the absence of the Co^{III} complex. Besides the progressive development of a coloration, starting from colourless reagents (Figure S20), monitoring this reaction by ^1H NMR and GC-MS gave clear indication that NEt_3 is able to reduce the benzoate radical to the benzoate anion. This is indirectly evidenced by the development new Et resonances plus a broad signal, which is assigned to an ammonium proton, in the ^1H NMR spectrum (Figure S21) and also by the presence of benzoic acid and diethyl benzamide in the GC trace (Figure S22). The benzamide must be formed within the GC column by condensation of $PhCOO^-H_2NEt_2^+$, because the ^1H spectrum does not show the expected benzamide resonances in solution. These results are strong indications in favour of the generation of diethylamine. Indeed, according to the literature, the monoelectronic oxidation of Et_3N leads to the formation of Et_2NH in the presence of water.[73] This experiment therefore suggests that a redox process occurs between BPO and NEt_3 to generate $PhCOO^-$ and $Et_3N^{+\bullet}$, the former yielding benzoic acid and the latter leading to a water-promoted decomposition to Et_2NH. A similar phenomenon is thus most likely occurring when the benzoate radical is generated by homolytic Co^{III}-O_2CPh bond cleavage from [$Co(acac)_2(O_2CPh)(NEt_3)$]. We anticipate that the initiation efficiency of [$Co^{III}(acac)_2(O_2CPh)$] in radical polymerization will be enhanced by ligands that, like Et_3N, are able to stabilize [$Co^{II}(acac)_2$] to a greater extent than [$Cp^{III}(acac)_2(O_2CPh)$], but cannot be oxidized by the benzoate radical. Investigations in this direction are in progress.

Conclusions

We have demonstrated that the general redox initiation approach of radical polymerisation by acyl peroxides, when using [$Co^{II}(acac)_2$] as the reducing activator and benzoyl peroxide as the initiator, implicates the generation of hitherto unreported but bench-stable [$Co^{III}(acac)_2(O_2Ph)$], the first mononuclear complex of Co^{III} with a carboxylate ligand and an entirely O-based coordination sphere. Adjustment of the [$Co^{II}(acac)_2$]/BPO stoichiometry to 2:1 constitutes a facile entry into this compound in good yields by a one-electron oxidative addition process, which proceeds *via* the generation of intermediate benzoate radicals. The Co^{III}-O bond to the benzoate ligand in this complex is sufficiently weak to allow this complex to be used as a unimolecular initiator of the controlled radical polymerisation of vinyl acetate, albeit with low initiation efficiencies due to the slow initiation relative to the reactivation of the weaker Co^{III}-C bond at the dormant chain end.

Author Contributions

MM; investigation, formal analysis, writing – original draft. JCD; investigation (X-ray diffraction). ASS; investigation (electrochemistry). CF, conceptualisation; funding acquisition; supervision; writing - review and editing. RP, conceptualisation; writing - review and editing.

Conflicts of interest

There are no conflicts to declare.

Acknowledgements

We gratefully acknowledge funding by the ANR (Agence Nationale de la Recherche) through the POLYSWITCH project (grant ANR-19-CE07-0031-01) and by the CNRS (Centre National de la Recherche Scientifique). RP is also grateful to the CALMIP mesocenter of the University of Toulouse for the allocation of computational resources.

Notes and references

1. F. P. Rotzinger and H. Li, *Inorg. Chem.*, 2018, **57**, 10122-10127.
2. D. A. Geselowitz, *Inorg. Chim. Acta*, 1988, **154**, 225.
3. R. C. Weast, *CRC Handbook of Chemistry and Physics*, CRC Press, Cleveland, Ohio, 57th edn., 2015.

4. H. A. Laitinen, A. J. Frank and P. Kivalo, *J. Am. Chem. Soc.*, 1953, **75**, 2865-2869.
5. I. Stein and U. Ruschewitz, *Z. Natuforsch. B*, 2011, **66**, 471-478.
6. Q. H. Li and S. W. Ng, *Acta Crystallogr. E*, 2010, **66**, M21-U316.
7. L. Martin, S. S. Turner, P. Day, P. Guionneau, J. A. K. Howard, D. E. Hibbs, M. E. Light, M. B. Hursthouse, M. Uruichi and K. Yakushi, *Inorg. Chem.*, 2001, **40**, 1363-1371.
8. V. M. Padmanabhan, *Proc. - Indian Acad. Sci., Sect. A*, 1958, **47A**, 329.
9. L. M. Shkolnikova and E. A. Shugam, *Zh. Strukt. Khim.*, 1961, **2**, 72.
10. P. K. Hon and C. E. Pfluger, *J. Coord. Chem.*, 1973, **3**, 67-76.
11. G. J. Kruger and E. C. Reynhardt, *Acta Crystallogr. B*, 1974, **30**, 822.
12. S. G. Patra, E. Illes, A. Mizrahi and D. Meyerstein, *Chem. Eur. J.*, 2020, **26**, 711-720.
13. I. Udachyan, T. Zidki, A. Mizrahi, S. G. Patra and D. Meyerstein, *ACS Applied Energy Materials*, 2022, **5**, 12261-12271.
14. A. I. Fisher, D. O. Ruzanov, N. S. Panina, A. N. Belyaev, S. A. Simanova, F. M. Dolgushin and A. V. Shchukarev, *Russ. J. Gen. Chem.*, 2008, **78**, 2006-2012.
15. Y. Sun, L. L. Zhu and H. H. Zhang, *Acta Crystallogr. E*, 2009, **65**, M1402-U1468.
16. J. K. Beattie, T. W. Hambley, J. A. Klepetko, A. F. Masters and P. Turner, *Chem. Commun.*, 1998, DOI: 10.1039/a707228g, 45-46.
17. A. I. Fischer, N. S. Panina and A. N. Belyaev, *Russian Journal of Coordination Chemistry*, 2016, **42**, 635-646.
18. E. G. Kastning, H. Naarmann, H. Reis and C. Berding, *Angew. Chem. Int. Ed.*, 1965, **77**, 322-327.
19. R. Thiagarajan, V. Kalpagam and U. S. Nandi, *J. Polym. Sci., Polym. Chem.*, 1982, **20**, 675-681.
20. G. Ferraudi, P. A. Grutsch and C. Kutal, *Inorg. Chim. Acta*, 1982, **59**, 249-253.
21. S. I. Dorovskikh, D. D. Klyamer, A. M. Makarenko, K. V. Zherikova, A. E. Turgambaeva, Y. V. Shevtsov, D. B. Kal'nyi, I. K. Igumenov and N. B. Morozova, *Vacuum*, 2022, **199**, 110969.
22. R. Poli, *Angew. Chem. Int. Ed.*, 2006, **45**, 5058–5070.
23. K. M. Smith, W. S. McNeil and A. S. Abd-El-Aziz, *Macromol. Chem. Phys.*, 2010, **211**, 10-16.
24. L. E. N. Allan, M. R. Perry and M. P. Shaver, *Progr. Polym. Sci.*, 2012, **37**, 127-156.
25. R. Poli, in *Polymer Science: A Comprehensive Reference*, eds. K. Matyjaszewski and M. Möller, Elsevier BV, Amsterdam, 2012, vol. 3, pp. 351–375.
26. J. Demarteau, A. Debuigne and C. Detrembleur, *Chem. Rev.*, 2019, **119**, 6906-6955.
27. A. Debuigne, R. Poli, C. Jérôme, R. Jérome and C. Detrembleur, *Prog. Polym. Sci.*, 2009, **34**, 211-239.
28. A. Debuigne, J. R. Caille and R. Jérôme, *Angew. Chem. Int. Ed.*, 2005, **44**, 1101-1104.
29. S. Maria, H. Kaneyoshi, K. Matyjaszewski and R. Poli, *Chem. Eur. J.*, 2007, **13**, 2480-2492.
30. A. Debuigne, C. Michaux, C. Jérôme, R. Jérôme, R. Poli and C. Detrembleur, *Chem. Eur. J.*, 2008, **14**, 7623-7637.
31. A. Debuigne, R. Poli, R. Jérôme, C. Jérôme and C. Detrembleur, *ACS Symp. Ser.*, 2009, **1024**, 131-148.
32. A. Debuigne, R. Poli, J. De Winter, P. Laurent, P. Gerbaux, J.-P. Wathelet, C. Jérôme and C. Detrembleur, *Macromolecules*, 2010, **43**, 2801-2813.
33. A. Debuigne, A. N. Morin, A. Kermagoret, Y. Piette, C. Detrembleur, C. Jérôme and R. Poli, *Chem. Eur. J.*, 2012, **18**, 12834–12844.
34. Y. Piette, A. Debuigne, C. Jérôme, V. Bodart, R. Poli and C. Detrembleur, *Polym. Chem.*, 2012, **3**, 2880-2891.
35. A. N. Morin, C. Detrembleur, C. Jérôme, P. D. Tullio, R. Poli and A. Debuigne, *Macromolecules*, 2013, **46**, 4303–4312.
36. A. Kermagoret, A. Debuigne, C. Jerome and C. Detrembleur, *Nat. Chem.*, 2014, **6**, 179-187.
37. Z. Wang, R. Poli, C. Detrembleur and A. Debuigne, *Macromolecules*, 2019, **52**, 8976-8988.
38. S. Banerjee, V. Ladmiral, A. Debuigne, C. Detrembleur, R. Poli and B. Améduri, *Angew. Chem. Int. Ed.*, 2018, **57**, 2934–2937.
39. P. G. Falireas, V. Ladmiral, A. Debuigne, C. Detrembleur, R. Poli and B. Ameduri, *Macromolecules*, 2019, **52**, 1266-1276.
40. B. B. Wayland, G. Poszmik and S. Mukerjee, *J. Am. Chem. Soc.*, 1994, **116**, 7943-7944.
41. B. B. Wayland, S. Mukerjee, G. Poszmik, D. C. Woska, L. Basickes, A. A. Gridnev, M. Fryd and S. D. Ittel, *ACS Symp. Ser.*, 1998, **685**, 305-315.
42. A. Debuigne, Y. Champouret, R. Jérôme, R. Poli and C. Detrembleur, *Chem. Eur. J.*, 2008, **14**, 4046-4059.
43. R. Bryaskova, C. Detrembleur, A. Debuigne and R. Jerome, *Macromolecules*, 2006, **39**, 8263-8268.
44. M. Hurtgen, A. Debuigne, C. Jerome and C. Detrembleur, *Macromolecules*, 2010, **43**, 886-894.
45. D. N. Bunck, G. P. Sorenson and M. K. Mahanthappa, *J. Polym. Sci., Polym. Chem.*, 2011, **49**, 242-249.
46. R. P. Nze, O. Colombani and E. Nicol, *J. Polym. Sci., Polym. Chem.*, 2012, **50**, 4046-4054.
47. G. S. Misra and U. D. N. Bajpai, *Prog. Polym. Sci.*, 1982, **8**, 61-131.
48. A. S. Sarac, *Progr. Polym. Sci.*, 1999, **24**, 1149-1204.
49. W. Kern, *Makromol. Chem.*, 1948, **1**, 249.
50. C. S. Marvel, R. Deanin, B. M. Kuhn and G. B. Landes, *J. Polym. Sci.*, 1948, **3**, 433.
51. A. Konishi and K. Nambu, *J. Polym. Sci.*, 1961, **54**, 209.
52. K. Dean, W. D. Cook, M. D. Zipper and P. Burchill, *Polymer*, 2001, **42**, 1345-1359.
53. M. Worzakowska, *J. Appl. Polym. Sci.*, 2006, **102**, 1870-1876.
54. A. C. Mortamet and R. A. Pethrick, *J. Appl. Polym. Sci.*, 2012, **123**, 1539-1547.
55. A. D. Jannakoudakis, C. Tsiamis, P. D. Jannakoudakis and E. Theodoridou, *Journal of Electroanalytical Chemistry*, 1985, **184**, 123-133.
56. J. Conradie, *Journal of the Electrochemical Society*, 2022, **169**.
57. C. J. Moody and G. H. Whitham, *Reactive Intermediates*, Oxford University Press, New York, 1992.
58. G. Moad and D. H. Solomon, *The Chemistry of free Radical Polymerization*, Elsevier, Amsterdam, 2nd edn., 2005.
59. W. N. S. Wing-Yiu Yu, Zhongyuan Zhou, and Albert S.-C. Chan, *Org. Lett.*, 2009, **11**, 3174-3177.
60. K. Fujimori, in *Organic Peroxides*, ed. W. Ando, Wiley, New York, 1992, p. 319.
61. C. Reichardt, J. Schroeder, P. Vohringer and D. Schwarzer, *Phys. Chem. Chem. Phys.*, 2008, **10**, 1662-1668.
62. F. A. Cotton and R. H. Holm, *J. Am. Chem. Soc.*, 1960, **82**, 2979-2983.

63. M. Michelas, C. Fliedel and R. Poli, in *Comprehensive Organometallic Chemistry IV*, Elsevier, 2021, vol. 1, ch. 1.03, pp. 31-85.
64. R. Poli, *C. R. Chimie*, 2021, **24**, 147-175.
65. R. G. Coombes and M. D. Johnson, *J. Chem. Soc. (A)*, 1966, 177-182.
66. A. R. Schmidt and T. W. Swaddle, *J. Chem. Soc. (A)*, 1970, 1927-1932.
67. R. S. Nohr and J. H. Espenson, *J. Am. Chem. Soc.*, 1975, **97**, 3392-3396.
68. G. W. Kirker, A. Bakac and J. H. Espenson, *J. Am. Chem. Soc.*, 1982, **104**, 1249-1255.
69. R. Morales-Cerrada, C. Fliedel, J.-C. Daran, F. Gayet, V. Ladmiral, B. Améduri and R. Poli, *Chem. Eur. J.*, 2019, **25**, 296-308.
70. K. S. Santhosh Kumar, Y. Gnanou, Y. Champouret, J.-C. Daran and R. Poli, *Chem. Eur. J.*, 2009, **15**, 4874-4885.
71. M. Döring, H. Görls and E. Uhlig, *Z. Anorg. Allg. Chem.*, 1991, **603**, 7-14.
72. P. Pauling, G. B. Robertson and G. A. Rodley, *Nature (London, U. K.)*, 1965, **207**, 73.
73. E. D. Cline, S. E. Adamson and S. Bernhard, *Inorg. Chem.*, 2008, **47**, 10378-10388.